Supporting Information

Modulating Central Metal Ions in Metal-Organic Cages for Enhanced CO_2 Photoreduction

Table of Content

1.Materials and Characterization Methods

All chemical reagents are used directly in their original state without the need for further purification. The main reagents used include: Tris (4-aminophenyl) amine ($C_{18}H_{18}N_4$, 97%, Bide Pharm), bis (trifluoromethylsulfonyl) imide cobalt ($C_4CoF_{12}N_2O_8S_4$, 98%, Bide Pharm), iron trifluoromethanesulfonate ($C_2F_6FeO_6S_2$, 98%, Bide Pharm), acetonitrile (C_2H_3N, 99%, Aladdin), and 2-pyridine formaldehyde (C_6H_5NO, 99%, Aladdin).

Structural characterization was performed using the following instruments: X-ray photoelectron spectroscopy (XPS) analysis was conducted on a VG ESCALAB MKII spectrometer (Thermo Fisher Scientific). Fourier transform infrared (FT-IR) spectra were obtained using a Nicolet 6700-FTIR spectrometer (Thermo Fisher Scientific). Electrochemical measurements were carried out on a CHI660 electrochemical workstation (CH Instruments). In situ attenuated total reflectance FTIR (in situ ATR-FTIR, Nicolet 6700-FTIR) was employed to monitor reaction intermediates. Optical absorption properties were evaluated via ultraviolet-visible (UV-Vis) spectroscopy (U-3900, Hitachi). Gas chromatography (GC-9720, Fuli Analytical) was used to quantify reaction products.

2.Experimental section

2.1 Synthesis of TNC@Co

Dissolve tris (4-aminophenyl) amine (9.0 mg, 31.1 μmol), bis (trifluoromethylsulfonyl) imide cobalt (21.5 mg, 31.1 μmol) and 2-pyridinaldehyde (10.0 mg, 93.3 μmol) in 2.5 ml of acetonitrile and ultrasonicate until dissolved. The reaction solution was stirred and reacted at 70 ℃ for 18 hours to obtain a deep orange solution. The reaction solution was concentrated to 1 ml, and an appropriate amount of ether was slowly added to precipitate a deep orange precipitate. Collect the sediment and wash it three times with ether to remove impurities. Finally, the precipitate was vacuum dried to obtain the target product in the form of a deep orange powder.

2.2 Synthesis of TNC@Fe

Tris (4-aminophenyl) amine (2.9 mg, 10 μmol), 2-pyridinaldehyde (2.85 μL, 30 μmol), iron trifluoromethanesulfonate (II) (3.54mg, 10 μmol) and acetonitrile (0.5 ml) were added to the reactor. The solution was degassed through three vacuum/nitrogen filling cycles, left overnight at 80 °C. After adding ethyl acetate, a purple powder precipitate was formed. The precipitate was filtered and rinsed with ethyl acetate, and then vacuum-dried to obtain the target product.

3.Photocatalytic Reduction of CO_2

Catalyst TNC@Co (2.0 mg), $[Ru(bpy)_3]Cl_2 \cdot 6H_2O$ (7.0 mg), and MeCN/ TEOA/ water (4:1:0.8,5.8 mL) were added to the optical reactor, and then pure carbon dioxide gas was introduced into the reactor for 10 minutes. The reaction temperature is maintained at 20 ℃. The reaction system was irradiated under a 300 W xenon lamp with an AM1.5G filter for 2 hours, and the products were detected by gas chromatography.

4.Photoelectrochemical property measurements

4.1 Preparation of the working electrode.

1 mg sample was dispersed in a mixture of 200 μL water, 200 μL ethanol, and 100 μL 0.5 wt% Nafion solution, and then sonicated to form a suspension. The prepared suspension (120 μL) was dispersed in an area of 1 × 1 cm^2 ITO substrate, and dried overnight at room temperature.

4.2 Photocurrent measurements.

The photoelectrochemical properties were tested in a standard three-electrode electrochemical cell via a CHI 660 electrochemical workstation, where the three electrodes include a working elec trode of 1 × 1 cm^2 ITO substrate supporting the catalyst, a counter electrode of the platinum plate, and a reference electrode of the saturated Ag/AgCl electrode. The electrolyte is 0.2 M sodium sulfate solution. The light source is 300 W Xe lamp equipped with an AM 1.5 filter.

4.3 Mott-Schottky measurements.

The Mott-Schottky plots were tested at different frequency (500 Hz, 800 Hz, 1000 Hz). The Mott-Schottky measurements were tested at a CHI 660 electrochemical workstation, where the electrolyte is 0.2 M sodium sulfate solution, the reference electrode is Ag/AgCl electrode, and the counter electrode is Pt plate. The semiconductor type will be determined from the C2 value vs. applied potential function relationship. A positive slope of the curve corresponds to an n-type semiconductor and vice versa for a p-type semiconductor.

5. Supplementary Figures

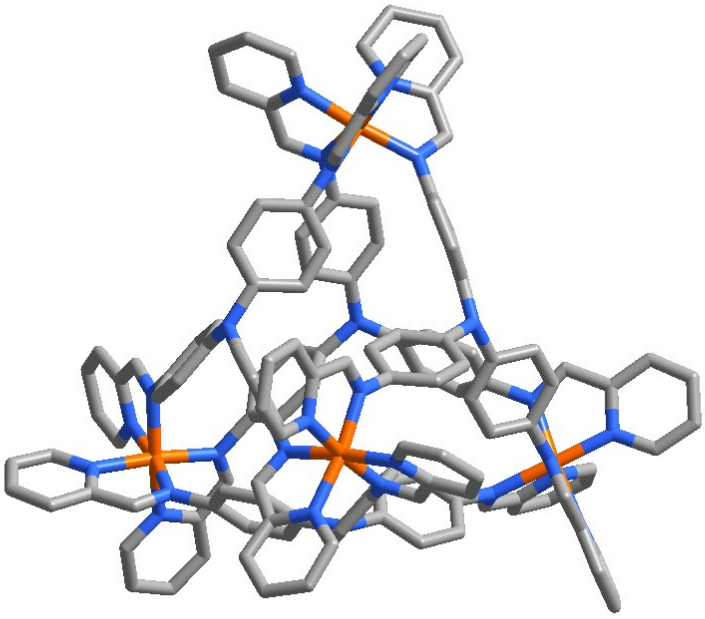

Fig. S1 Structural Diagram of TNC@Co.

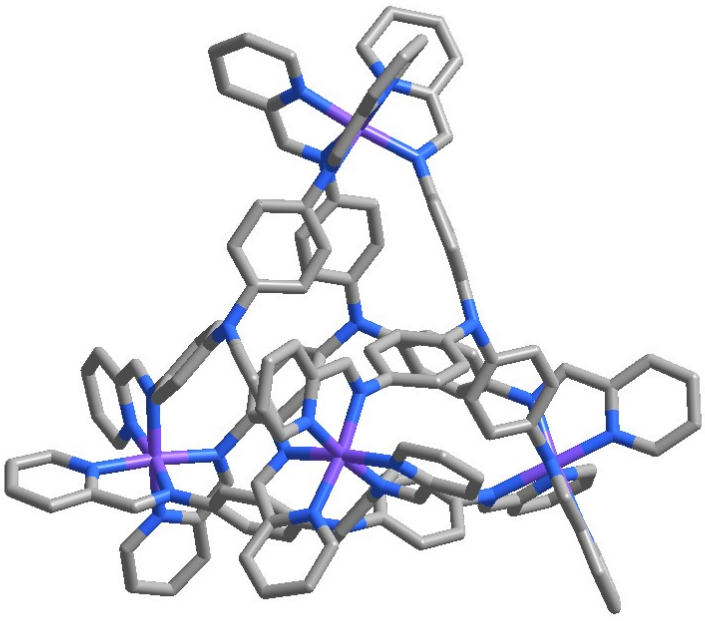

Fig. S2 Structural Diagram of TNC@Fe.

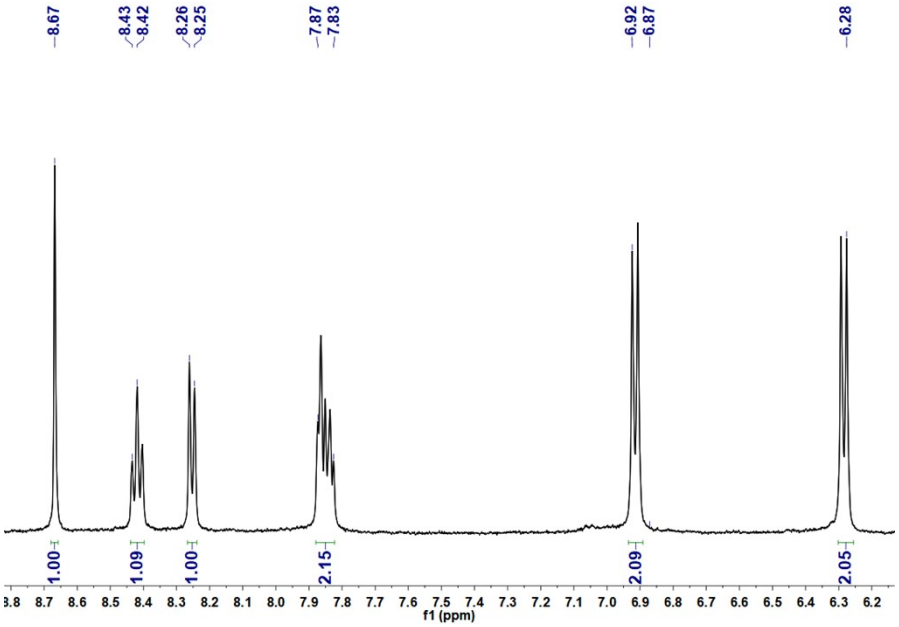

Fig. S3 ^{1}H NMR spectrum of TNC@Fe.

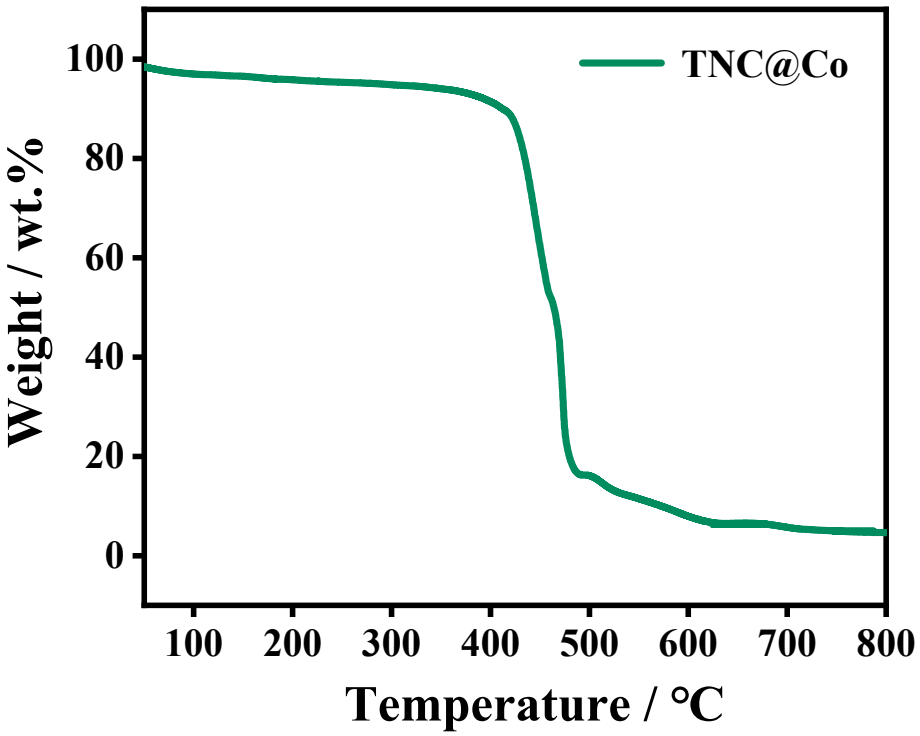

Fig. S4 TGA of TNC@Co.

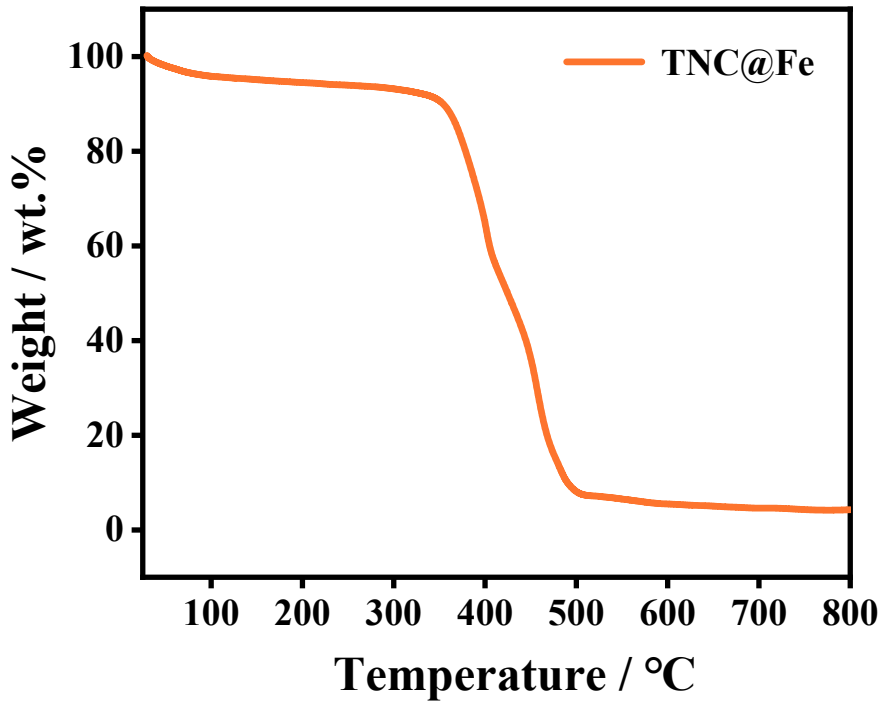

Fig. S5 TGA of TNC@Fe.

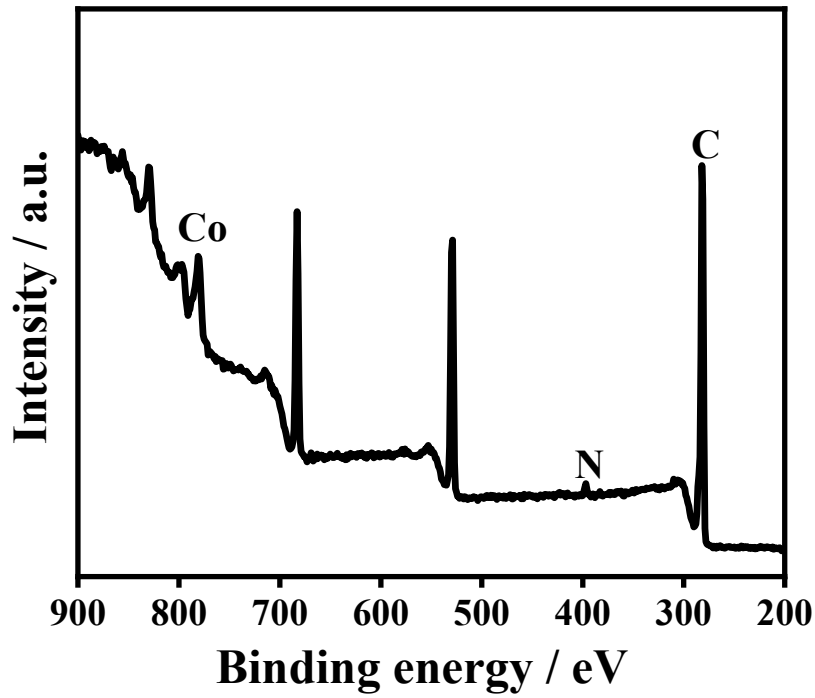

Fig. S6 XPS survey spectrum of TNC@Co.

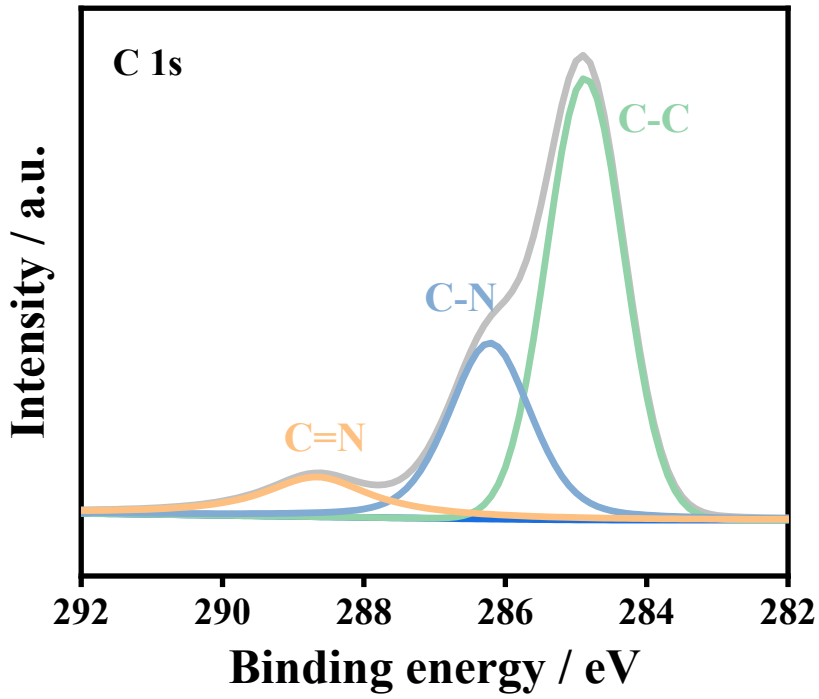

Fig. S7 High-resolution XPS spectrum of C 1s for TNC@Co.

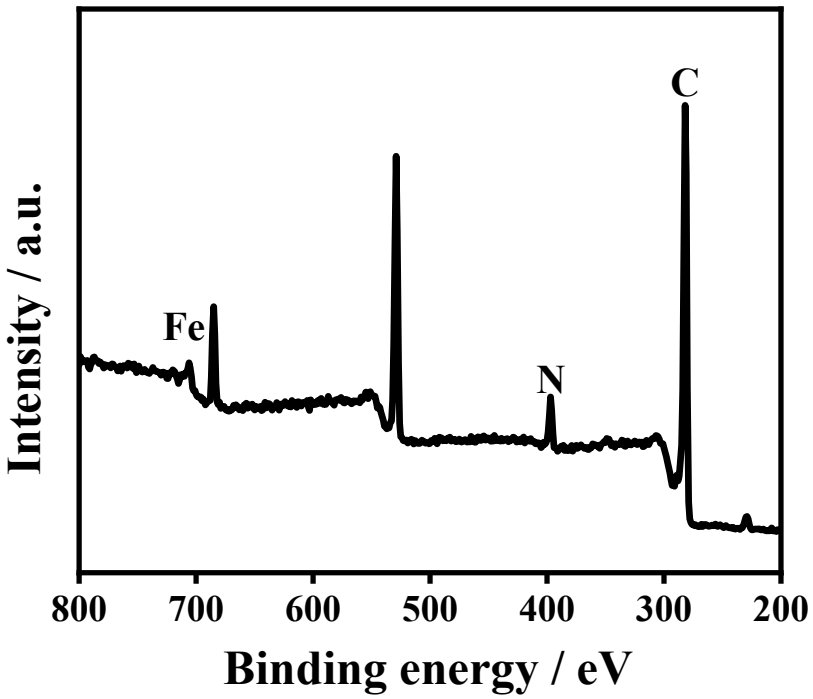

Fig. S8 XPS survey spectrum of TNC@Fe.

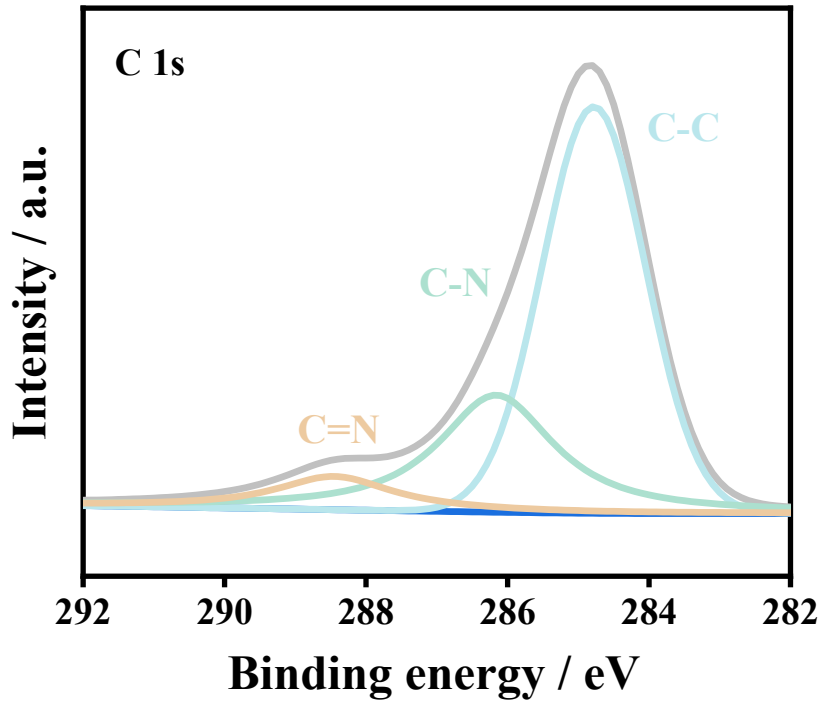

Fig. S9 High-resolution XPS spectrum of C 1s for TNC@Fe.

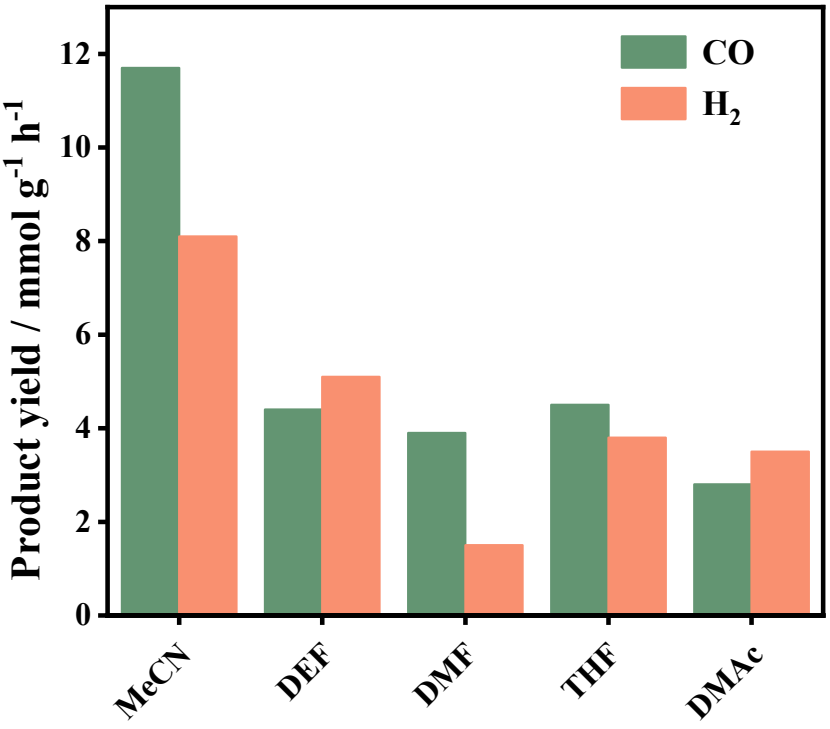

Fig. S10 Effect of different solvents on photocatalytic performance.

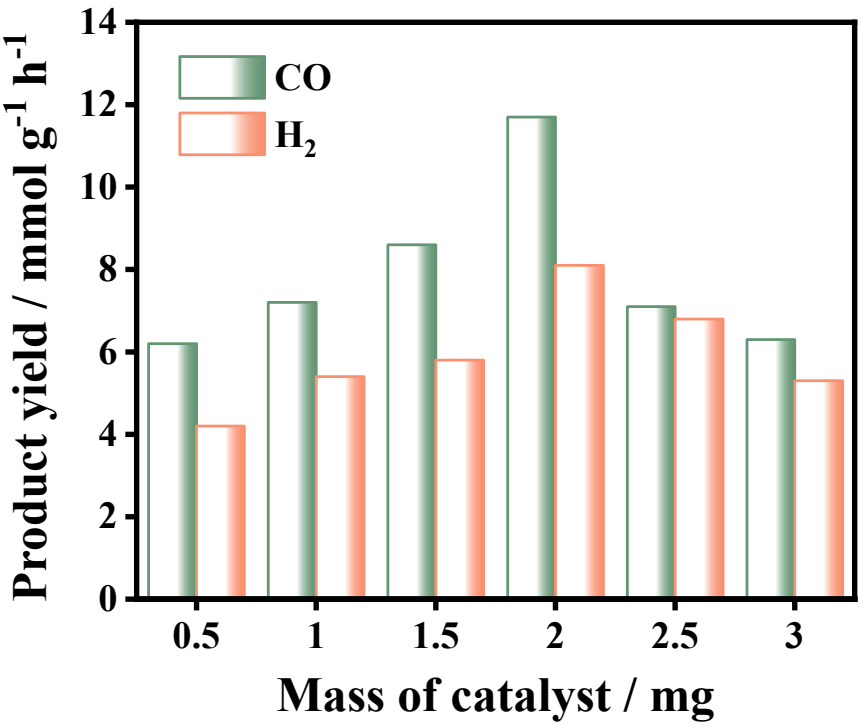

Fig. S11 Effect of TNC@Co dosage on photocatalytic performance.

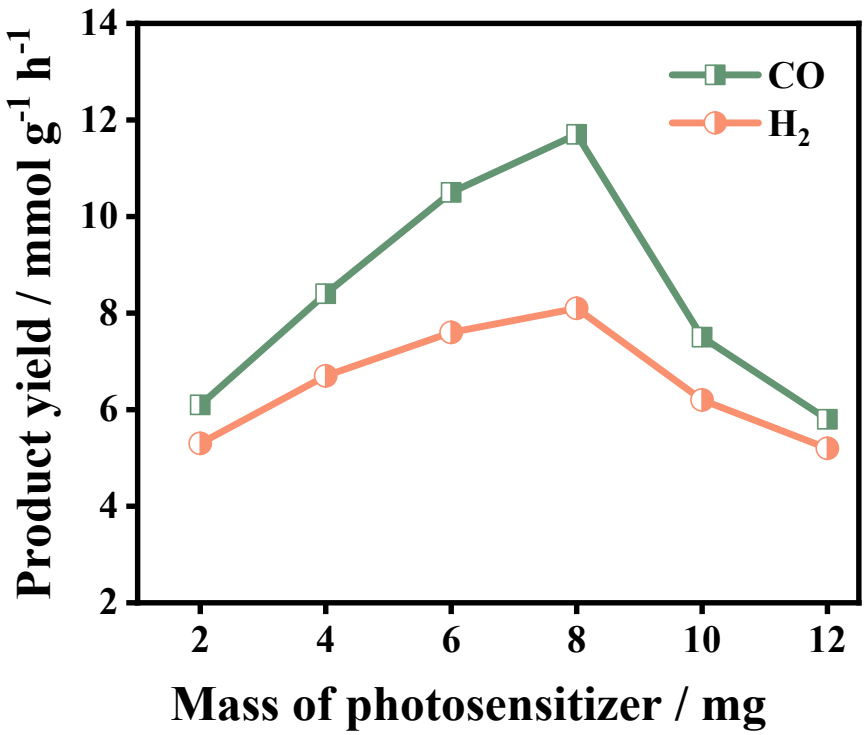

Fig. S12 Effect of photosensitizer dosage on photocatalytic performance.

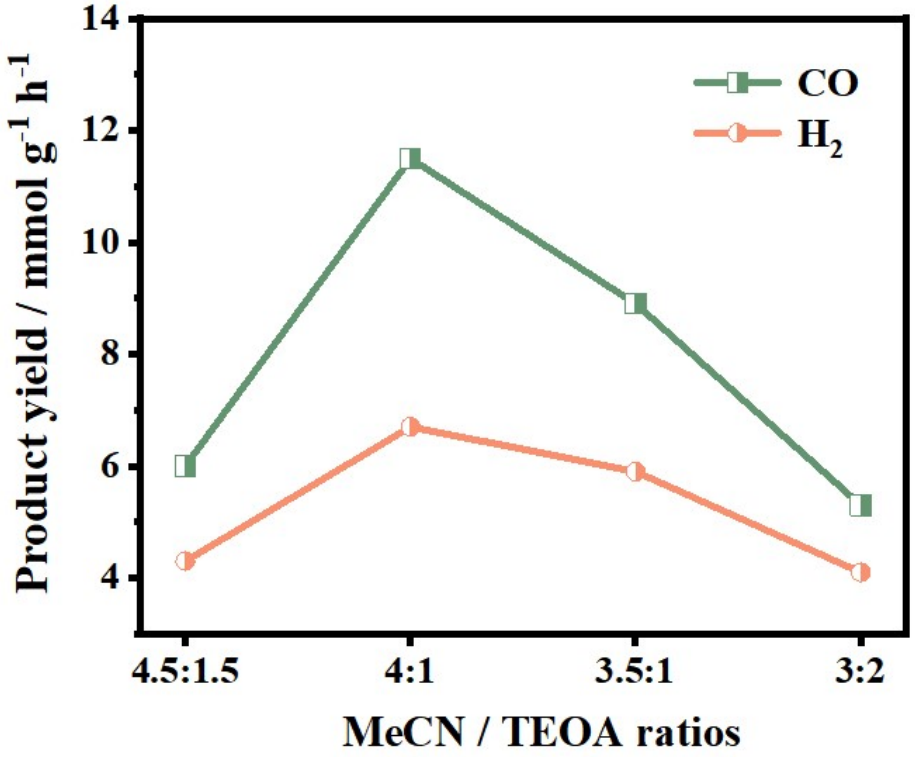

Fig. S13 The Effect of the Acetonitrile and TEOA Ratio on Photocatalytic Performance.

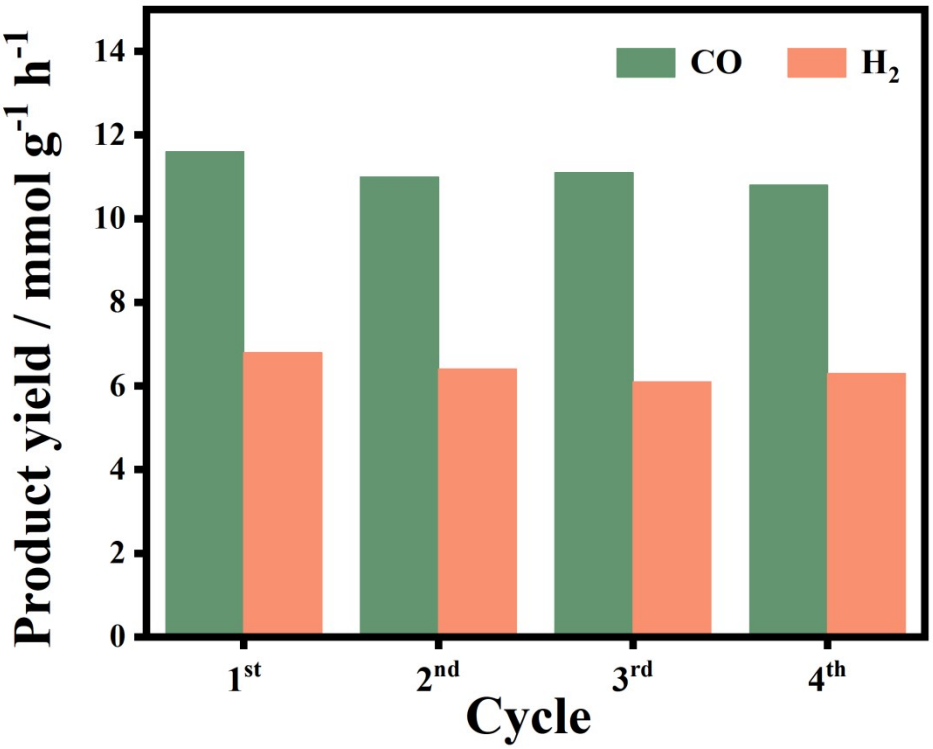

Fig. S14 Photocatalytic cycle testing of TNC@Co.

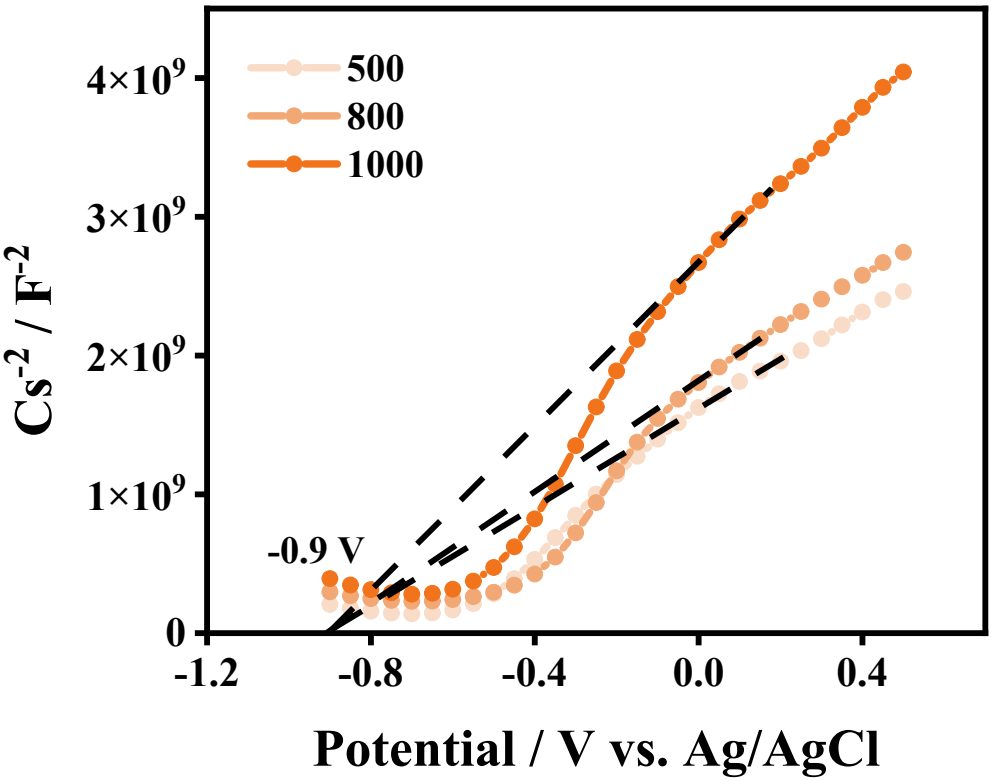

Fig. S15 Mott-Schottky plots of TNC@Fe.

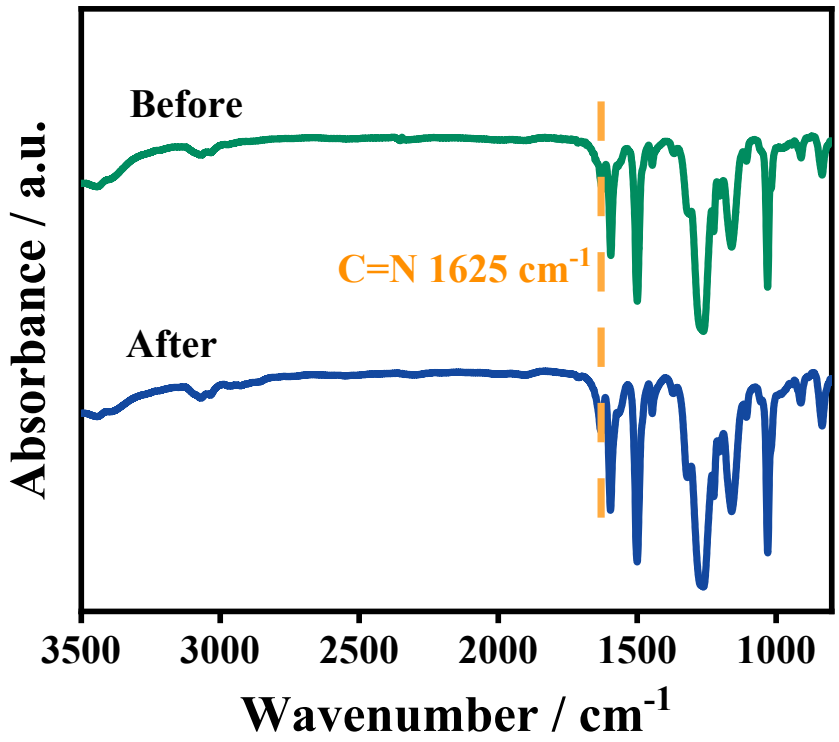

Fig. S16 FTIR spectra of TNC@Co.

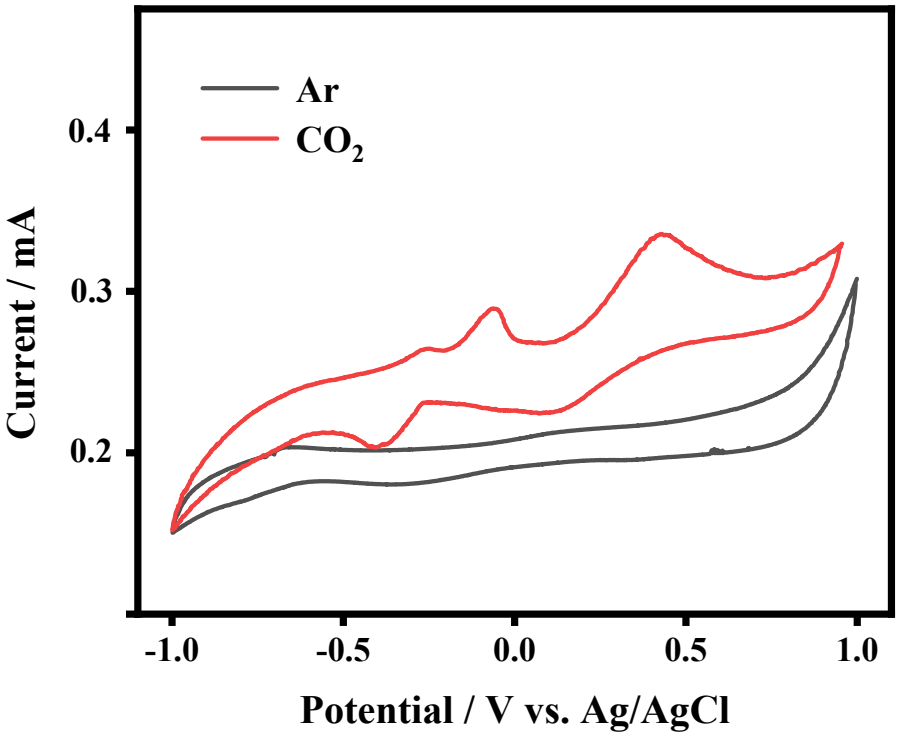

Fig. S17 CV Curve Testing of TNC@Co in Ar and CO_2 Atmospheres.

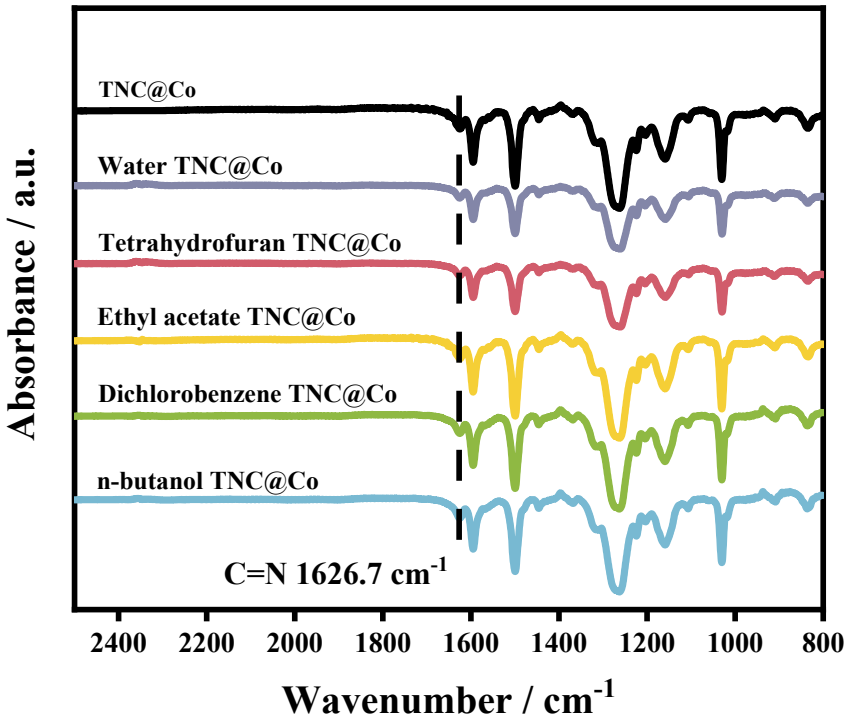

Fig. 18 FTIR spectra of TNC@Co in different solvents.

Table S1 Comparison of Photocatalytic CO_2 Reduction Performance Between TNC@Co and similar materials.

Photocatalysts	Product	CO Generation Rate	Ref.
TNC@Co	CO/H_2	11.7 mmol g^{-1} h^{-1}	this work
BIF-29	CO/H_2	3.334 mmol g^{-1} h^{-1}	[1]
ZrT-1-NH_2-IS-Co	CO/H_2	7.3 mmol g^{-1} h^{-1}	[2]
ReP/TiO_2-MOC-Q2	CO/H_2	0.604 mmol g^{-1} h^{-1}	[3]
MOC-18N	CO/H_2	MOC-18N:3.848 mmol g^{-1} h^{-1}	[4]
MOC-24N		MOC-24N:3.517 mmol g^{-1} h^{-1}	
MOC-36N		MOC-36N:3.935 mmol g^{-1} h^{-1}	
CoFe-PBA	CO/H_2	3.49 mmol g^{-1} h^{-1}	[5]
PTC-373-Co	CO/H_2	0.970 mmol g^{-1} h^{-1}	[6]
PTC-391-Cu	CO/H_2	0.668 mmol g^{-1} h^{-1}	
$Ni_8L_{12}I_4$	CO/H_2	2.68 mmol g^{-1} h^{-1}	[7]
$Ni_8L_{12}Br_4$	CO/H_2	0.5964 mmol g^{-1} h^{-1}	
$Ni_8L_{12}Cl_4$	CO/H_2	0.01202 mmol g^{-1} h^{-1}	
Schiff-base ZrOC-1	CO/H_2	2.55 mmol g^{-1} h^{-1}	[8]

6. Reference

1. H.-X. Zhang, Q.-L. Hong, J. Li, F. Wang, X. Huang, S. Chen, W. Tu, D. Yu, R. Xu, T. Zhou and J. Zhang, *Angewandte Chemie International Edition*, 2019, **58**, 11752-11756.
2. J. He, M. Dong, Y. Zhao, J. Gu, C. Sun, D. Cui, X. Yao, F. Meng, C. Tao, X. Wang and Z. Su, *Chinese Chemical Letter*s, 2026, **3**7, 111253.
3. S. Qin, Y. Lei, J.-F. Huang, C.-Y. Lv, X.-A. Li, P.-Y. Su and J.-M. Liu, *ACS Sustainable Chemistry & Engineering*, 2022, **10**, 8254-8264.
4. M.-T. Lv, M.-D. Cui, K.-P. Bai, Y. Jiang, W.-P. Chen, N.-N. Sun, X.-Q. Hu, C. Huang, Q.-Y. Yang and Y.-Z. Zheng, *Angewandte Chemie International Edition*, 2025, **64**, e202506838.
5. Y. Zheng, Y. Zeng, S. Lu, H. Huang, Z. Zhuang and Y. Yu, *Small*, 2025, **21**, e06220.
6. Y.-F. Li, Y.-P. He, X. Xie, G.-H. Chen, H.-X. Zhang and J. Zhang, *Inorganic Chemistry*, 2025, **64**, 24362-24367.
7. L. Huang, L. Qin, S. Wan, Y. Yan, S. Cao, J. Zhang and T. Zhou, *Angewandte Chemie International Edition*, 2025, **64**, e202509280.
8. J. He, M. Dong, Y. Zhao, D. Cui, X. Yao, F. Meng, W. Li, S. Yang, C. Sun and Z. Su, *Inorganic Chemistry Frontiers*, 2024, **11**, 5120-5126.